Eurographics/ ACM SIGGRAPH Symposium on Computer Animation (2009)
E. Grinspun and J. Hodgins (Editors)

Anisotropic Friction for Deformable Surfaces and Solids

Simon Pabst and Bernhard Thomaszewski and Wolfgang Straßer

Graphical-Interactive Systems (GRIS)
Wilhelm Schickard Institute for Computer Science, Tübingen, Germany
{pabst,b.thomaszewski,strasser}@gris.uni-tuebingen.de

Abstract

This paper presents a method for simulating anisotropic friction for deforming surfaces and solids. Frictional contact is a complex phenomenon that fuels research in mechanical engineering, computational contact mechanics, composite material design and rigid body dynamics, to name just a few. Many real-world materials have anisotropic surface properties. As an example, most textiles exhibit direction-dependent frictional behavior, but despite its tremendous impact on visual appearance, only simple isotropic models have been considered for cloth and solid simulation so far. In this work, we propose a simple, application-oriented but physically sound model that extends existing methods to account for anisotropic friction. The sliding properties of surfaces are encoded in friction tensors, which allows us to model frictional resistance freely along arbitrary directions. We also consider heterogeneous and asymmetric surface roughness and demonstrate the increased simulation quality on a number of two- and three-dimensional examples. Our method is computationally efficient and can easily be integrated into existing systems.

Categories and Subject Descriptors (according to ACM CCS): Computer Graphics [I.3.5]: Physically based modeling—Computer Graphics [I.3.7]: Three-Dimensional Graphics and Realism—, Animation

Keywords: computer animation, cloth simulation, physics based animation, friction

1. Introduction

Friction is a ubiquitous phenomenon. Whenever surfaces touch, friction acts as a force that resists tangential motion between the objects in contact. Because of this, it is of vital importance to model frictional effects in physically based animations of, e.g., cloth or volumetric solids.

Research into friction has a long history. Scientists such as da Vinci, Amontons and Coulomb were the first in the attempt to understand this complex effect. They concluded empirically that friction force is

- directly proportional to the applied normal pressure force (*Amontons 1st Law*)
- independent of the apparent area of contact (*Amontons 2nd Law*)
- independent of the sliding velocity (*Coulomb's Law of Friction*): $\mathbf{F}_f = \mu \mathbf{F}_n$,

where μ is the dimensionless friction coefficient and $\mathbf{F}_n$ is the normal pressure force.

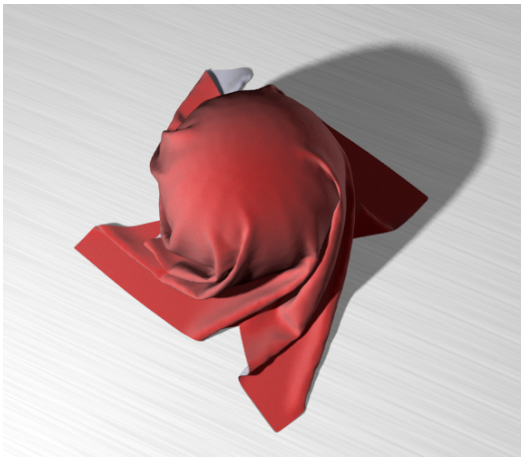

Figure 1: *Friction plays an important role in the formation of wrinkles and folds.*

These laws describe *dry friction*, which further distinguishes between two contact scenarios: *static* friction, which acts only during resting contact, and *kinetic* or *sliding* friction, which is only active in case of nonzero relative motion between contact regions.

Although much more sophisticated models have been proposed in later literature (refer to section 2), this empirically derived model enjoys widespread use in computer graphics. Reasons for this are its ease of implementation, computational efficiency and reasonably realistic results. However, many common materials such as textiles, biological tissue, wood, engineered surfaces and many more, exhibit anisotropic surface roughness — and this direction-dependent behavior cannot be captured with an isotropic model. Friction forces for anisotropic and heterogenous materials do not only depend on normal pressure and a single friction coefficient, but also on the sliding direction and the spatial location of contact. Unlike in the isotropic setting, the friction force is not necessarily oriented along the sliding direction. This leads to much more complex frictional behavior and effects which are largely beyond the range of what conventional models predict.

Physically based simulation in computer graphics has since long taken anisotropic material properties into account. For example, cloth simulation relies on orthotropic materials to model the yarn structure of textiles [VMT05, TPS09] and volumetric solids simulation often deals with highly anisotropic materials, e.g., biological tissues [PDA03, TBHF03]. While great attention is given to anisotropy in materials models, so far only simple isotropic friction models have been considered.

Goals and Contributions

In this paper, we propose a model of generalized dry Coulomb friction in the anisotropic domain, a natural continuation of the trend to anisotropic material models. Our method also accounts for heterogeneous, i.e., spatially varying surface friction and friction asymmetry. The new approach seamlessly integrates into standard simulation frameworks and it can conveniently replace the simpler friction model used in [BFA02]. The technique is applicable to both elastic surfaces, like cloth or shells, and volumetric solids, like soft tissue or rubber. Our method has only slightly higher computational costs than isotropic approaches and the additional effort is generously rewarded by a variety of interesting new effects.

Before discussing our method in detail (Sec. 3), we first summarize relevant related work.

2. Related Work

Measuring and computing friction forces on various types of surfaces is an important problem in many engineering applications. Studies into friction anisotropy can be traced back to the 18th century, when Coulomb and others examined the influence of the orientation of wooden surfaces on the sliding direction [Cou21].

Frictional Contact Mechanics The works on friction in the physics, engineering and applied mathematics communities are far too numerous to be cited in full here. We therefore focus on publications that are specifically concerned with anisotropic friction models. Recent work includes Konyukhov et al. [KVS08], who discuss a numerical model for anisotropic contact interfaces including adhesion and friction. Our approach is inspired by Zmitrowicz's tensorial model of anisotropic friction as described in [Zmi81, Zmi06]. Cirak and West [CW05] present a contact response model for explicit finite element simulations including isotropic frictional contacts. Many textiles show strongly anisotropic friction characteristics and Howell et al. [HMT59] summarize much of the earlier work in the field of textile sciences. A standard for measuring friction properties experimentally was established later as a part of the Kawabata Evaluation System [Kaw80].

Friction in Computer Graphics The pioneering work of Terzopoulos et al. [TPBF87] already laid out how to include frictional effects in computer graphics simulations. Isotropic Coulomb-Amontons friction models are used for many applications including, e.g., cloth simulation in the widely-used framework by Bridson et al. [BFA02]. This technique was later extended by Selle et al. [SSIF09] retaining isotropy, however. Harmon et al. [HVTG08] approximate isotropic Coulomb friction in their simultaneous collision handling approach. Otaduy et al. [OTSG09] recently presented a method for handling collisions inside implicit time integration using Lagrange multipliers. However, they use a simple 4-sided polygonal pyramid as a linear approximation of the isotropic friction cone.

Contact is also a well-studied problem in rigid body simulation. Baraff published a series of papers (e.g., [Bar91, Bar93]) on dealing with static and dynamic friction in Linear Complementarity Problem (LCP) solvers. Mirtich and Canny [MC95] use microcollisions in their impulse-based rigid body dynamics system and include a friction model. Irving et al. [ITF04] use a variation of the Bridson-framework for 3D deformable solids simulations.

To the best of our knowledge, no attempt to model anisotropic, asymmetric and heterogeneous friction has been reported in the computer graphics literature so far.

3. Friction Model

Beyond the microscopic scale, we can safely assume that the bounding surfaces of colliding objects are smooth. Then, if two points $\mathbf{p}_a$ and $\mathbf{p}_b$ are in contact, the infinitesimal surface patches surrounding them have exactly opposite normal directions. Hence, there is a tangential contact plane, which

induces a decomposition of relative motion $\mathbf{v}_{rel}$ into *normal* and *tangential* velocity, $\mathbf{v}_n$ and $\mathbf{v}_t$ (see Fig. 2). Friction forces occur only if the relative motion between the contacting regions is nonzero: normal motion leads to (or is opposed by) normal pressure, which determines the magnitude of friction force. Tangential motion determines the direction of friction force but does not affect its magnitude.

Collisions and Friction In the context of computer graphics, most of the methods apply friction during collision handling, which bears direct practical appeal. For the sake of efficiency, all collisions are treated simultaneously at the end of the time step (a notable exception being the recent work by Harmon et al. [HVS*09]). This motivates the widely used velocity filter approach by Bridson et al. [BFA02]: assuming that contact forces $\mathbf{F}_n$ are constant during a time step, they can be computed as a function of the collision-resolving impulse $m\Delta\mathbf{v}_n = \int_t^{t+\Delta t} \mathbf{F}_n \, dt = \mathbf{F}_n \Delta t$, which cancels out relative motion in normal direction. $\mathbf{F}_n$ can then be used to compute friction forces from the remaining tangential velocity, and an equivalent tangential correction $\Delta\mathbf{v}_t$ is determined as

$$\Delta\mathbf{v}_t = \max(1 - \mu\frac{\Delta\mathbf{v}_n}{|\mathbf{v}_t|}, 0)\mathbf{v}_t \ . \tag{1}$$

Eq. 1 models isotropic static and sliding Coulomb friction in a very efficient way and we therefore adopt it as the basis for our extensions to the anisotropic, asymmetric and heterogeneous setting.

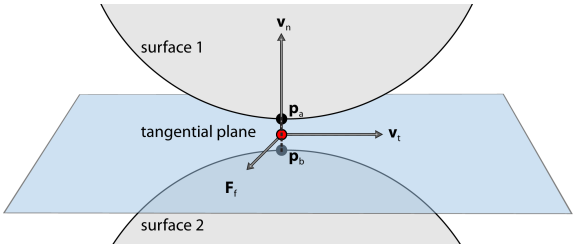

Figure 2: *A contact point between two surfaces. Relative velocity is decomposed into tangential and normal components.*

Anisotropy and Orientation Anisotropic friction is characterized by the fact that the friction force depends not only on normal pressure and a single friction coefficient (as in the case of Coulomb friction) but also on the sliding direction. To be able to identify the sliding direction, a parametrization of the involved surfaces is needed. Local coordinate systems are conveniently established in each point of the surfaces using existing texture coordinates (*uv*-parametrization). For a given vertex with normal $\mathbf{n}$, we compute tangent vectors $\mathbf{t}$ and $\mathbf{b}$ aligned with texture-space directions u and v respectively, such that $[\mathbf{t}, \mathbf{b}, \mathbf{n}]$ defines an orthonormal basis, i.e., $\mathbf{n} = \mathbf{t} \times \mathbf{b}$.

In order to compute friction forces, we first need to identify the points of contact on the two surfaces (or single surface, in case of self-collisions). In the discrete setting, this amounts to finding geometric primitive pairs in close proximity. As many other approaches, we handle only vertex-triangle and edge-edge primitive pairs. For each of these pairs we compute the basis frames $[\mathbf{t}_i, \mathbf{b}_i, \mathbf{n}_i]$ for $i = 0, 1$ at the actual point of contact, interpolating vertex frames inside triangles by barycentric weighting. Although the contact normals coincide in the continuous setting (see above) this is not necessarily so in the discrete case: e.g. the face normal of a vertex-triangle pair will generally be different from the vertex normal and edge-edge collisions can either be treated using their cross-product or the vector between the pair of closest points on them. The concrete choice is, however, not important as long as the same normal $\mathbf{n}_c$ is used for both primitives. For simplicity, we can assume that the contact normal coincides with the normal of the first surface and we subsequently rotate the local coordinate frame of the second system into this contact plane. This transformation renders $[\mathbf{t}_1, \mathbf{b}_1]$ and $[\mathbf{t}_2, \mathbf{b}_2]$ coplanar while keeping their relative orientation unchanged. From this orientation, which is determined by the angle $\varphi = \text{acos}(\mathbf{t}_1 \cdot \mathbf{t}_2)$, we can define the rotation matrix

$$\mathbf{R} = \begin{bmatrix} \cos(\varphi) & -\sin(\varphi) \\ \sin(\varphi) & \cos(\varphi) \end{bmatrix} \ , \tag{2}$$

which aligns the friction tensors $\mathbf{Q}_1$ and $\mathbf{Q}_2$ of the two surfaces appropriately. We obtain the unit-length tangential sliding velocity $\hat{\mathbf{v}}_t$ by projecting the relative velocity $\mathbf{v}_{rel}$ of the contact points onto the contact plane and normalizing. Finally, the anisotropic friction force $\bar{\mathbf{F}}_f$ for sliding direction $\hat{\mathbf{v}}_t$ is computed as

$$\bar{\mathbf{F}}_f = -\mathbf{F}_n \kappa (\mathbf{Q}_1 + \mathbf{R}^t \mathbf{Q}_2 \mathbf{R}) \hat{\mathbf{v}}_t \ , \tag{3}$$

where $\mathbf{F}_n$ is the normal pressure force and κ is the friction composition coefficient [Zmi81]. While κ is a material dependent parameter that can actually be measured for a given combination of surfaces in contact, we prefer to reduce complexity and set $\kappa = 0.5$ in the remainder of the paper. Eq. (3) describes the effective friction tensor as an additive composition of the two surface tensors. This may not necessarily be the best choice in the context of computer animation, since setting one of the tensors to zero does not result in the probably expected zero friction force. If such behavior is desired, a multiplicative or minimum composition law is better suited.

$\bar{\mathbf{F}}_f$ is a vector in the tangential contact plane and needs to be transformed back to the world space vector $\mathbf{F}_f$ as

$$\begin{bmatrix} F_{f,x} \\ F_{f,y} \\ F_{f,z} \end{bmatrix} = \begin{bmatrix} t_{1,x} & b_{1,x} & n_{c,x} \\ t_{1,y} & b_{1,y} & n_{c,y} \\ t_{1,z} & b_{1,z} & n_{c,z} \end{bmatrix} \cdot \begin{bmatrix} \bar{F}_{f,x} \\ \bar{F}_{f,y} \\ 0 \end{bmatrix} \ . \tag{4}$$

From $\mathbf{F}_f$ we can now easily compute velocity-correcting impulses as outlined in [BFA02]. We limit the impulses so that the change in relative tangential velocity $\Delta\mathbf{v}_t$ is not larger than the pre-friction velocity $\Delta\mathbf{v}_t^{pre}$ (see Eq. (1)). In this way, we also model static friction, i.e., the case of vanishing slip velocity.

Physical soundness requires the preservation of linear and angular momentum, i.e., friction must not introduce any net force or torque. The former follows immediately since the forces for the contact points are of equal magnitude but opposite direction, $\mathbf{F}_{f,1} = -\mathbf{F}_{f,2}$. The second requirement is met by assuring that friction forces act only in the tangential contact plane [CW05].

3.1. Anisotropic Friction Models

The friction tensor $\mathbf{Q}$ maps tangential motion to forces in the tangent plane. It is therefore a 2×2-tensor and we write

$$\mathbf{Q} = \begin{bmatrix} Q_{11} & Q_{12} \\ Q_{21} & Q_{22} \end{bmatrix}$$

As a fundamental constraint, physical principles (2^{nd} law of thermodynamics) dictate that the friction force be dissipative, which translates into a determinant $\det \mathbf{Q} = Q_{11}Q_{22} - Q_{12}Q_{21} \geq 0$. While an extensive discussion of further restrictions can be found in [Zmi06], we focus on the three types with most practical interest, which are

- isotropic friction: $Q_{11} = Q_{22}$, $Q_{12} = Q_{21} = 0$ and $Q_{11} \geq 0$,
- orthotropic friction: $Q_{12} = Q_{21}$ and $Q_{11} \geq 0$, and
- fully anisotropic friction.

Heterogenous Friction Many materials have inhomogeneous roughness characteristics, for example due to a mosaic-like structure or the effects of wear. We can easily extend our approach to represent this interesting behavior by modulating the friction tensor $\mathbf{Q}$ of a surface with a simple 4-channel texture map:

$$\mathbf{Q} = \begin{bmatrix} r_{uv}Q_{11} & g_{uv}Q_{12} \\ b_{uv}Q_{21} & a_{uv}Q_{22} \end{bmatrix} \tag{5}$$

where $[r_{uv}, g_{uv}, b_{uv}, a_{uv}]$ are the 4 color values of the texture at the current point of contact, in the range of $[0,1]$. Instead of taking a single sample of the friction texture at the beginning or end of the time step, we integrate the texture values over Δt, assuming a linear sliding path and contact during the entire time step. This approach gave slightly improved results in our test cases, especially with sharp changes in the texture.

Asymmetric Friction The approach described so far is *symmetric* in the sense that the resulting friction force is invariant under rotations of $n \cdot \pi$ of the sliding direction. A broad class of materials does, however, not obey this behavior. Examples include animal fur or many types of carpets, where the oriented fibers lead to increased resistance in one direction, and far less in the opposing direction. This effect is called *friction asymmetry*.

We can extend our model to materials for which the friction force depends on the sense of the sliding direction by introducing a second friction tensor. Although more complex models are possible, we restrict our considerations to cases in which the material behavior for opposing directions is completely decoupled. In this case, the material can be described by two tensors $\mathbf{Q}^+$ and $\mathbf{Q}^-$ modeling frictional properties in positive and negative sense along two main directions $\mathbf{r}$ and $\mathbf{v}$.

Figure 3: *Ratchet structure (cf. [Zmi06])*

For the sake of simplicity, we assume that $\mathbf{r}$ and $\mathbf{v}$ are orthogonal to each other. Without loss of generality we further assume that $\mathbf{r}$ and $\mathbf{v}$ coincide with the material basis vectors. In order to ease the derivation of asymmetric material behavior, we temporarily resort to 4-dimensional space: decomposing the tangential velocity as $\mathbf{v}_t = \mathbf{v}^+ + \mathbf{v}^-$, we introduce $\tilde{\mathbf{v}} = [\mathbf{v}_x^+, \mathbf{v}_y^+, \mathbf{v}_x^-, \mathbf{v}_y^-]^t$, with

$$\mathbf{v}_x^+ = \begin{cases} \mathbf{v}_{t,x} & , \mathbf{v}_{t,x} > 0 \\ 0 & , \textit{otherwise} \end{cases}$$

and accordingly for the other components. Note that this additive decomposition induces two disjoint two-dimensional subspaces in $\mathbf{R}^4$. Letting $\mathbf{Q}^+$ and $\mathbf{Q}^-$ denote the material's friction tensors for positive and negative sliding directions, we can now write

$$\tilde{\mathbf{F}} = \begin{bmatrix} \mathbf{Q}^+ & \mathbf{0} \\ \mathbf{0} & \mathbf{Q}^- \end{bmatrix} \cdot \tilde{\mathbf{v}} \,. \tag{6}$$

where $\tilde{\mathbf{F}} = [\mathbf{F}_x^+, \mathbf{F}_y^+, \mathbf{F}_x^-, \mathbf{F}_y^-]^t$. The forces in the two-dimensional tangent plane are then obtained by projecting $\mathbf{F} = [\mathbf{F}_x^+ + \mathbf{F}_x^-, \mathbf{F}_y^+ + \mathbf{F}_y^-]^t$. Note that this model accurately separates the material behavior for positive and negative sliding directions, while naturally satisfying first-order continuity requirements for the transitions between the two senses.

This extension can be used to model a multitude of interesting phenomena, e.g. the effect of many tiny hairs on human skin, which affect the behavior of clothing. They cause asymmetric frictional behavior, which manifests for example in the sleeves of shirts, which slide more easily downwards on the arms than upwards.

4. Results

4.1. Cloth simulation

We integrated the proposed approach into a standard cloth simulation system based on finite element membrane forces and the discrete-shell model of Grinspun et al. [GHDS03]. We use a semi-implicit backward Euler scheme for time integration [BW98] and handle collisions within a velocity filter framework similar to the one proposed by [BFA02]. This makes the integration of our new model as a replacement for the isotropic friction computation straightforward.

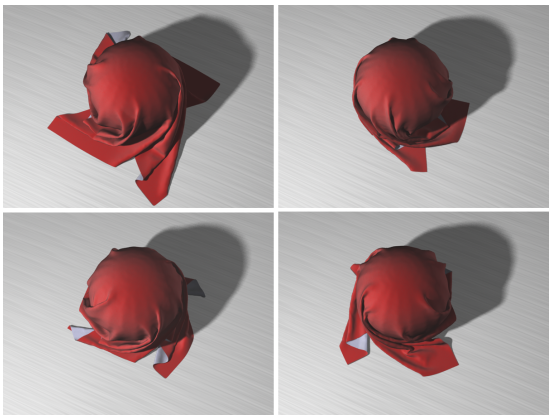

Figure 4: *Piece of cloth (*$2.5m \times 2.5m$*,* 14.000 *faces) draped over a rotating sphere. Top row: anisotropic cloth, bottom row: isotropic cloth.*

Fig. 4 visualizes the effects of anisotropic friction on a piece of cloth draped over a rotating sphere. The top row shows anisotropic friction for counterclockwise and clockwise rotation, respectively, while the bottom row displays the results with purely isotropic friction. The cloth in the top row drapes very differently depending on the rotation direction, since both cloth-rigid contacts and self-contacts are influenced by the anisotropic roughness. The isotropic simulations in the bottom row, not surprisingly, look very much alike, since the change in rotation direction does not lead to different friction forces. Figures 5 and 6, respectively, demonstrate heterogeneous and asymmetric frictional behavior. The full simulations can be found in the accompanying video.

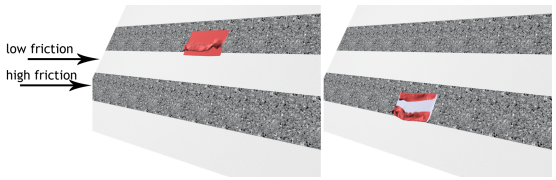

Figure 5: *Fabric piece (*$1m \times 1m$*,* 1.500 *faces) sliding down an inclined plane with heterogeneous roughness. The textured stripes are* $10\times$ *rougher than the untextured area. The textile topples over as it enters the high friction region, but continues to slide downwards, since the cloth-cloth friction is relatively low.*

4.2. Volumetric solids simulation

Our approach is not limited to cloth simulation and we also integrated it into our finite element based volumetric solids simulation system. Collision handling works on the surface meshes and is mostly identical to the cloth simulation framework. Fig. 7 shows the combined simulations of soft spheres rolling down an inclined plane. We ran several simulations with varying degrees of anisotropy on the plane. Anisotropic friction results in deviating sliding directions and also deforms the spheres into cigarillo-like shapes, the stronger the anisotropy, the stronger the effect. This very simple example already clearly demonstrates the increased simulation quality that can be achieved by including friction anisotropy. Behavior such as this could not be represented using isotropic friction alone.

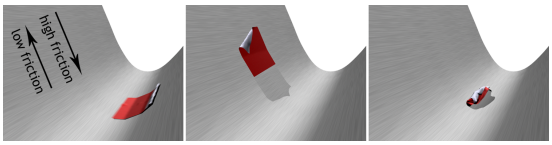

Figure 6: *Piece of cloth (*$1m \times 1m$*,* 1.500 *faces) sliding down a half-pipe structure. The surface roughness is asymmetric - in sliding direction right to left it exhibits low friction, but in the opposing direction it has high friction coefficients.*

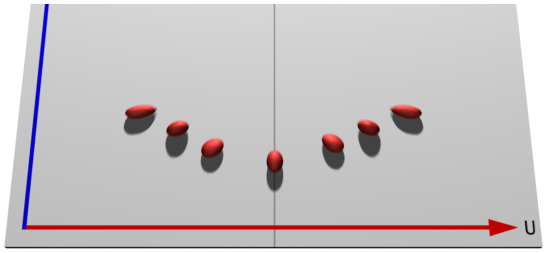

Figure 7: *Soft volumetric spheres (2.164 tetrahedra each) rolling down an inclined plane. Anisotropic friction deforms the spheres into cigarillo-like shapes, much different from the isotropic friction model used with the central sphere.*

4.3. Performance

To examine the performance impact compared to isotropic models, we created a simple but representative test scene. A piece of cloth (1.000 faces, $1m \times 1m$) slides down an inclined plane (40° inclination, $5m \times 5m$). The textile is in full contact with the plane during the whole simulation.

	$t_{collision}$	$t_{friction}$	$\%_{friction}$
no friction	6.5s	–	–
[BFA02] (isotropic)	7.3s	0.7s	10%
our model (anisotropic)	8.7s	2.2s	25%

Table 1: *Comparison of computation times in seconds, for* $1s$ *of simulation using a time step of* $\Delta t = 1ms$.

The results show that anisotropic friction is only slightly more expensive than the simpler isotropic model. This is due to the additional coordinate system transformations and trigonometric functions used in evaluating the relative surface orientations.

5. Conclusion

We presented a fully anisotropic friction model for deformable objects simulation. The technique is simple to implement, efficient and can easily be integrated into standard simulation frameworks. We described two extensions of anisotropic behavior that allowed us to simulate heterogeneous surface roughness and asymmetric friction. A variety of 2D cloth and 3D volumetric solids examples attest to the potential of anisotropic friction to improve simulation results.

Limitations One limitation of our approach is the increased number of input parameters it needs when compared to the single, intuitive friction coefficient μ in the isotropic model. μ-values for a great number of material combinations can be found in standard textbooks, while there is not nearly as much data available regarding anisotropic roughness. The situation is not unlike the one for other simulation parameters, e.g., anisotropic elastic moduli data for tissue samples is also hard to come by. However, our approach behaves in a very comprehensible fashion, and as such it is not difficult to come up with parameters that model a desired effect, especially for the purposes of computer animation.

We use the *uv*-parametrization of objects to identify relative orientations. Finding a suitable set of *uv*-coordinates can be a non-trivial task with complex 3D shapes.

Future Work While the model described in this paper improves the state-of-the-art, it does by no means include all aspects of frictional behavior. We simulate *dry friction*, while excluding the effects of *wet friction*. The interaction of lubricated surfaces is an interesting field for further work, especially with publications like [LAD08], which recently made the efficient simulation of wet porous objects possible.

Another interesting project would be the inclusion of electrostatic phenomena induced by frictional contacts.

Furthermore, it could be worthwhile to integrate anisotropic friction into [OTSG09], i.e., as part of the implicit solve.

References

[Bar91] BARAFF D.: Coping with friction for non-penetrating rigid body simulation. In *SIGGRAPH '91* (1991), pp. 31–41.

[Bar93] BARAFF D.: Issues in computing contact forces for non-penetrating rigid bodies. *Algorithmica 10*, 2-4 (1993), 292–352.

[BFA02] BRIDSON R., FEDKIW R., ANDERSON J.: Robust treatment of collisions, contact and friction for cloth animation. In *SIGGRAPH '02* (2002), pp. 594–603.

[BW98] BARAFF D., WITKIN A.: Large steps in cloth simulation. In *SIGGRAPH '98* (1998), pp. 43–54.

[Cou21] COULOMB C. A.: *Theorie des machines simples: en ayant egard au frottement de leurs parties et a la roideur des cordages*. Bachelier, 1821.

[CW05] CIRAK F., WEST M.: Decomposition-based contact response (DCR) for explicit finite element dynamics. *International Journal for Numerical Methods in Engineering 64* (2005), 1078–1110.

[GHDS03] GRINSPUN E., HIRANI A., DESBRUN M., SCHRÖDER P.: Discrete shells. In *SCA '03* (2003), pp. 62–67.

[HMT59] HOWELL H. G., MIEZKIS K. W., TABOR D.: *Friction in Textiles*. Textile Book Publishers, 1959.

[HVS*09] HARMON D., VOUGA E., SMITH B., TAMSTORF R., GRINSPUN E.: Asynchronous Contact Mechanics. *SIGGRAPH '09* (2009).

[HVTG08] HARMON D., VOUGA E., TAMSTORF R., GRINSPUN E.: Robust Treatment of Simultaneous Collisions. *SIGGRAPH '08* (2008).

[ITF04] IRVING G., TERAN J., FEDKIW R.: Invertible finite elements for robust simulation of large deformation. In *SCA '04* (2004), pp. 131–140.

[Kaw80] KAWABATA S.: *The Standardization and Analysis of Hand Evaluation*. The Textile Machinery Society of Japan, Osaka, 1980.

[KVS08] KONYUKHOV A., VIELSACK P., SCHWEIZERHOF K.: On coupled models of anisotropic contact surfaces and their experimental validation. *Wear 264*, 7-8 (2008), 579–588.

[LAD08] LENAERTS T., ADAMS B., DUTRÉ P.: Porous flow in particle-based fluid simulations. In *SIGGRAPH '08* (2008).

[MC95] MIRTICH B., CANNY J.: Impulse-based simulation of rigid bodies. In *SI3D '95* (1995), pp. 181–190.

[OTSG09] OTADUY M., TAMSTORF R., STEINEMANN D., GROSS M.: Implicit Contact Handling for Deformable Objects. In *Eurographics '09* (2009).

[PDA03] PICINBONO G., DELINGETTE H., AYACHE N.: Nonlinear anisotropic elasticity for real-time surgery simulation. *Graph. Models 65*, 5 (2003), 305–321.

[SSIF09] SELLE A., SU J., IRVING G., FEDKIW R.: Robust high-resolution cloth using parallelism, history-based collisions, and accurate friction. *IEEE TVCG 15*, 2 (2009), 339–350.

[TBHF03] TERAN J., BLEMKER S., HING V. N. T., FEDKIW R.: Finite volume methods for the simulation of skeletal muscle. In *SCA '03* (2003), pp. 68–74.

[TPBF87] TERZOPOULOS D., PLATT J., BARR A., FLEISCHER K.: Elastically deformable models. In *SIGGRAPH '87* (1987), pp. 205–214.

[TPS09] THOMASZEWSKI B., PABST S., STRASSER W.: Continuum-based Strain Limiting. In *Eurographics '09* (2009).

[VMT05] VOLINO P., MAGNENAT-THALMANN N.: Accurate garment prototyping and simulation. *Computer-Aided Design & Applications 2*, 5 (2005), 645–654.

[Zmi81] ZMITROWICZ A.: A Theoretical Model of Anisotropic Dry Friction. *Wear 73* (1981), 9–39.

[Zmi06] ZMITROWICZ A.: Models of kinematics dependent anisotropic and heterogeneous friction. *International Journal of Solids and Structures 43*, 14-15 (2006), 4407–4451.